Bmp8a Is a Novel Player in Regulation of Antiviral Immunity

Shenjie Zhong, Haoyi Li, Yun-Sheng Wang, Ying Wang, Guangdong Ji, Hong-Yan Li, Shicui Zhang*, Zhenhui Liu**

1 College of Marine Life Science and Institute of Evolution & Marine Biodiversity, Ocean University of China, Qingdao 266003, China

2 Laboratory for Marine Biology and Biotechnology, Pilot National Laboratory for Marine Science and Technology (Qingdao), Qingdao 266003, China

*Correspondence author: e-mail: sczhang@ouc.edu.cn

**Correspondence author: e-mail: zhenhuiliu@ouc.edu.cn

Abstract

Bone morphogenetic protein (BMP) is a kind of classical multi-functional growth factor that plays a vital role in the formation and maintenance of bone, cartilage, muscle, blood vessels, and the regulation of energy balance. Whether BMP plays a role in antiviral immunity is unknown. Here we demonstrate that Bmp8a is a newly-identified positive regulator for antiviral immune responses. The *bmp8a*$^{-/-}$ zebrafish, when infected with the viruses of GCRV, SVCV or TSVDV, show significantly reduced antiviral immunity, increased viral load and morbidity. We also show for the first time that Bmp8a interacts with Alk6a, which promotes the phosphorylation of Tbk1 and Irf3 through p38 MAPK pathway, and induces the production of type I IFNs in response to virus infection. Upon virus infection, *bmp8a* expression is activated through the binding of Stat1a/Stat1b to the GAS motifs in *bmp8a* promoter region, enlarging the antiviral innate immune signal. Our study uncovers a previously unrecognized role of Bmp8a in regulation of antiviral immune responses and provides a new target for controlling viral infection.

Introduction

Viruses infect all groups of living things and produce a variety of diseases. Host cell detection of viral infection depends on the recognition of pathogen-associated molecular patterns (PAMPs) from viral proteins or nucleic acids by the pattern recognition receptors (PRRs) such as Toll-like receptors (TLRs), RIG-I-like receptors (RLRs), NOD-like receptors (NLRs) and cytoplasmic DNA or RNA sensors[1-6]. The PRRs, once stimulated by their appropriate ligands, trigger distinct intracellular signaling pathways that converge on the activation of IFN regulatory factor 3 (IRF3) and/or IFN regulatory factor 7 (IRF7), which then translocate into the nucleus and activate the production of interferons (IFNs) that play important roles in inhibiting virus replication[7,8].

IFNs are classified into type I IFNs that include IFNα and IFNβ; type II IFN which has only a single member IFN-γ; and type III IFNs that consist of IFN-λs[9]. All these three types of IFNs trigger intracellular signaling cascades generally via the Janus kinase signal transducer and activator of transcription (JAK-STAT) pathway[10]. Canonically, type I IFNs initiate the signaling via binding to a heterodimeric receptor complex IFN-α/β receptor (IFNAR), inducing phosphorylation of transcription factors STAT1 and STAT2. The phosphorylated STATs form a trimolecular complex with IRF9, which translocates to the nucleus and binds to IFN-stimulated response elements (ISREs) of IFN-stimulated genes (ISGs), resulting in transcriptional activation of the target ISGs, including those encoding numerous cytokines and antiviral proteins[11-16]. In contrast, type II IFN binds to its unique receptor, IFN-γ receptor (IFNGR), resulting in the phosphorylation of STAT1 and the formation of STAT1 homodimers that recognize gamma-activated sequences (GASs) present in the promoter regions of IFN-γ-regulated genes[9].

Bone morphogenetic proteins (BMPs) are potent growth factors belonging to the transforming growth factor beta (TGFβ) superfamily, which are intercellular signaling molecules with multiple functions in development and differentiation, such as skeletal formation and hematopoiesis, as well as lipid oxidation[17-21]. However, accumulating data suggests that BMPs also play important roles in the regulation of immune responses[22-27]. For example, BMP7 has been shown to drive Langerhans cell differentiation[28]. Interestingly, BMP signaling appears to have different responses in T cells: BMP4 and BMP6 were shown to promote T cell proliferation, whereas BMP2 was seen to inhibit T cell proliferation[29,30]. In addition, although BMPs were found to promote tumor growth by inhibiting the functions of cytotoxic T lymphocytes (CTLs) and dendritic cells (DCs), they were also shown to inhibit cancer cell proliferation and promote the activity of NK cells that typically display antitumour activity[31]. Therefore, it remains controversial regarding the functions of BMPs in immune responses.

In humans and mice, two closely related BMP8 genes, *BMP8A* and *BMP8B*, have been identified[32,33]. BMP8B has been found to play roles in the regulation of thermogenesis in mature brown adipose tissue and spermatogenesis in male germ cells, while BMP8A shown to closely correlate with the progression of spermatogenesis[34,35]. In contrast, only one

93 *bmp8* gene, *bmp8a*, has been isolated in zebrafish, and shown to be involved in the regulation of lipid metabolism[36]. To
94 date, whether Bmp8a plays a role in immune responses is completely unknown. The present study was thus performed
95 to answer this question. We demonstrated that Bmp8a was a previously unrecognized regulator functioning in antiviral
96 immune responses of zebrafish *Danio rerio*, providing a new target for control of viral infection.
97

98 **Results**

99 **Bmp8a inhibited RNA virus replication *in vitro*.** To explore the function of zebrafish Bmp8a in the antiviral immune
100 response, we infected both the wild-type zebrafish liver (ZFL) cells and ZFL cells over-expressing bmp8a as well as the
101 epithelioma papulosum cyprini (EPC) cells and EPC cells over-expressing bmp8a with Grass carp reovirus (GCRV), a
102 dsRNA virus, and then monitored the cytopathic effect（CPE）and the viral titers of the supernatants. In response to GCRV
103 challenge, an apparent CPE was observed in the control cells, while the bmp8a-overexpressing ZFL cells had much less
104 CPE (Fig. 1a). In accordance with the CPE results, a significant decrease of the viral titers was observed in the
105 supernatants of bmp8a-overexpressing ZFL cells (Fig. 1b). Similarly, the GCRV-induced CPE and GCRV yields of the
106 supernatants were also markedly reduced in the bmp8a-overexpressing EPC cells (Fig. 1c, d). These suggested that
107 Bmp8a suppressed the replication of the RNA virus in the cells.
108

109 **Bmp8a was involved in antiviral responses *in vivo*.** To test the function of Bmp8a in host defense against virus infection
110 *in vivo*, we generated *bmp8a* deficient (*bmp8a*$^{-/-}$) zebrafish using the TALEN approach (Supplementary Fig. 1a), which
111 caused 7 nucleotides deletion in the exon 4 (Supplementary Fig. 1b, c). We challenged both the wild-type and *bmp8a*$^{-/-}$
112 mutant zebrafish by intraperitoneal injection with GCRV. Compared with wild-type zebrafish, the levels of GCRV RNA in
113 the liver, kidney, intestine, and spleen of *bmp8a*$^{-/-}$ zebrafish were considerably increased (Fig. 1e). Accordingly, *bmp8a*$^{-/-}$
114 zebrafish exhibited significantly reduced survival rate than wild-type zebrafish upon GCRV infection (Fig. 1f). When the
115 wild-type and *bmp8a*$^{-/-}$ zebrafish were similarly challenged with spring viremia of carp virus (SVCV), a negative ssRNA
116 virus, the survival rate of *bmp8a*$^{-/-}$ zebrafish was also remarkably lower than that of wild-type zebrafish (Fig. 1g). Moreover,
117 when the wild-type and *bmp8a*$^{-/-}$ zebrafish were infected with turbot skin verruca disease virus (TSVDV) isolated from
118 skin (Supplementary Fig. 2), mortality occurred in *bmp8a*$^{-/-}$ zebrafish at 108 h postinfection, and all the fish died at 156 h
119 post infection, while none of the wild type zebrafish were dead during the period (Fig. 1h). These data indicated that
120 *bmp8a*$^{-/-}$ zebrafish were more susceptible to virus infection than wild-type zebrafish, suggesting involvement of Bmp8a in
121 antiviral immune responses *in vivo*.

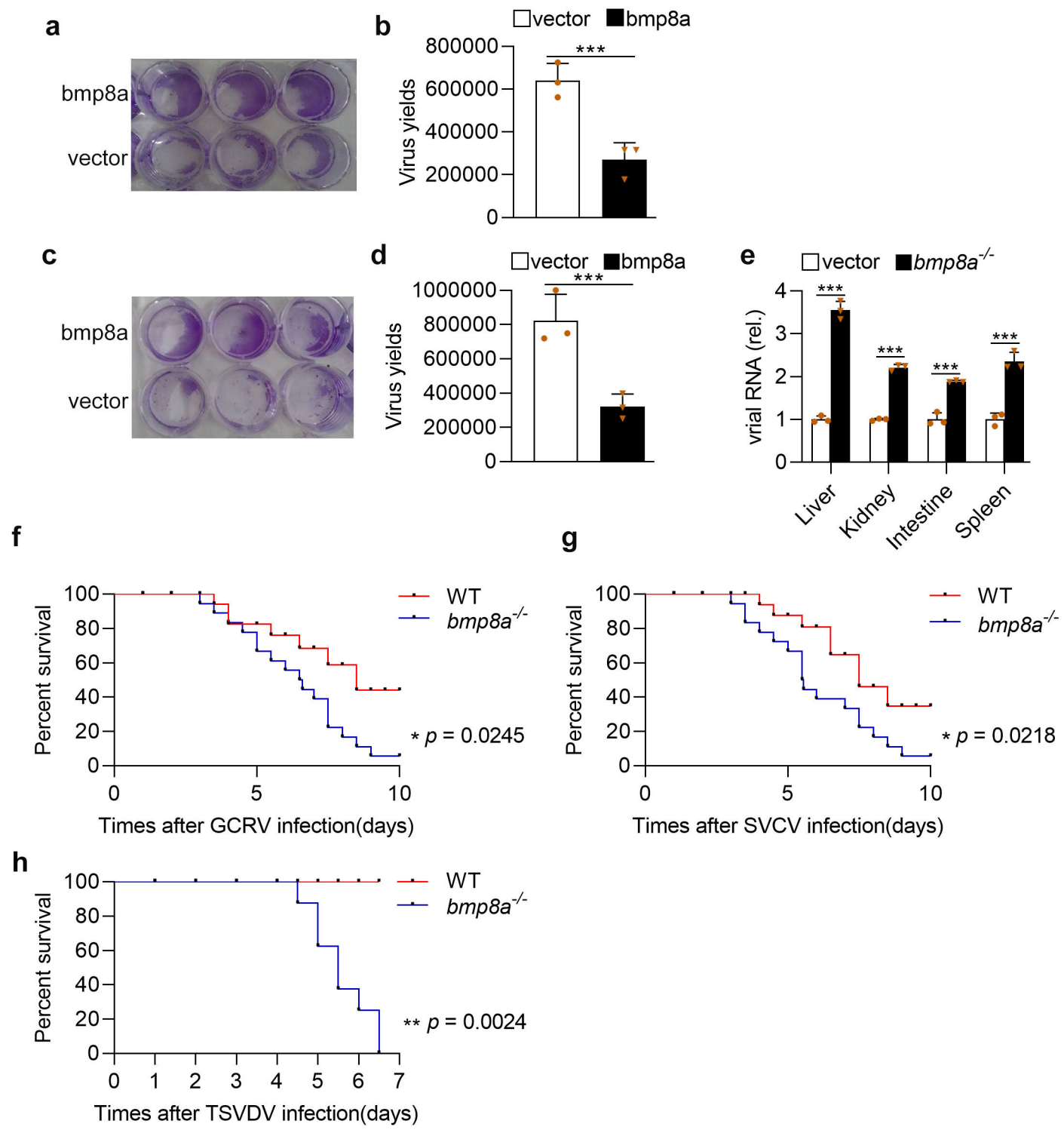

Fig.1 Bmp8a inhibits RNA virus replication both *in vitro* and *in vivo*. a, **b** ZFL cells were transfected with bmp8a (1μg) or empty vector (1μg), respectively. The cells were infected with GCRV (5×10^4TCID$_{50}$ per ml) at 24 h post-transfection, and the culture supernatants were collected at 72 h post-infection. The cell monolayers were fixed with 4% paraformaldehyde for 1 h and stained with 0.5% crystal violet for 2 h (**a**), and the viral titers of the supernatants were determined by TCID$_{50}$ assays (**b**). **c**, **d** Similar as (**a**, **b**) but in EPC cells. **e** The expression of GCRV RNA in the liver, kidney, intestine, and spleen from wild-type (WT) or *bmp8a*$^{-/-}$ zebrafish injected i.p. with 50 μl of GCRV (10^8TCID$_{50}$ per ml) for 72 h. **f**, **g** Kaplan–Meier analysis of the overall survival of WT (n = 20) or *bmp8a*$^{-/-}$ zebrafish (n = 20) which were injected i.p. with 50 μl of GCRV (10^8TCID$_{50}$ per ml) or SVCV (10^8TCID$_{50}$ per ml) and monitored every 12 h after infection. **h** Kaplan–Meier analysis of the overall survival of WT (n = 8) or *bmp8a*$^{-/-}$ zebrafish (n = 8) which were injected i.p. with 50 μl of TSVDV (crude virus extracts filtered by a 0.45 μm microporous membrane) and monitored every 12 h after infection. The expression of zebrafish *actb1* was used as an internal control for the qRT-PCR. Data were from three independent experiments (**a–e**) or two independent experiments (**f-h**). Data were analyzed by Student's *t*-test (two-tailed) or log-rank

135 (Mantel–Cox) test and were presented as mean ± SD (*$p < 0.05$, ***$p < 0.001$). Source data are provided as a Source
136 Data file.
137
138 **Bmp8a promoted expression of antiviral genes.** In zebrafish, type I IFNs contained 4 members *ifnφ1*, *ifnφ2*, *ifnφ3*, and
139 *ifnφ4*, among which *ifnφ1* and *ifnφ3* were shown to be involved in the antiviral response. In contrast, in carp, only one type
140 I IFN was identified to fulfill antiviral role in EPC cell[37,38]. To pinpoint the role of Bmp8a in the antiviral immune response,
141 both the wild-type and *bmp8a*$^{-/-}$ zebrafish were injected intraperitoneally with GCRV, and the expression of type I IFN
142 genes and the antiviral protein gene *mx* were detected using quantitative reverse transcription PCR (qRT-PCR). We found
143 that the expression of both *ifnφ1* and *ifnφ3* as well as *mx* was all significantly down-regulated in the liver, kidney, intestine,
144 and spleen of *bmp8a*$^{-/-}$ zebrafish, compared with those of wild-type fish (Fig. 2a-d). We then over-expressed bmp8a in
145 ZFL cells and found that ZFL cells with over-expressed Bmp8a showed markedly higher expression of *ifnφ1*, *ifnφ3*, and
146 *mx* than that of control cells, infected with or without GCRV (Fig. 2e-h). In addition, *bmp8a* knockdown caused remarkably
147 decreased expression of *ifnφ1*, *ifnφ3*, and *mx* in ZFL cells (Fig. 2i-l). Similarly, the expression of *ifn* and *mx* in EPC cells
148 with over-expressed Bmp8a was also remarkably up-regulated than that in control cells (Fig. 2m-p). Moreover, EPC cells
149 cotransfected with bmp8a expressing plasmid and IFNφ1, IFNφ3, or EPC IFN promoter-driven luciferase plasmid, followed
150 by infection with or without GCRV, had markedly increased intracellular IFNφ1, IFNφ3, or EPC IFN promoter-driven
151 luciferase activities (Fig. 2q-s). All these data denoted that Bmp8a promoted the expression of both type I IFN and *mx*
152 genes.

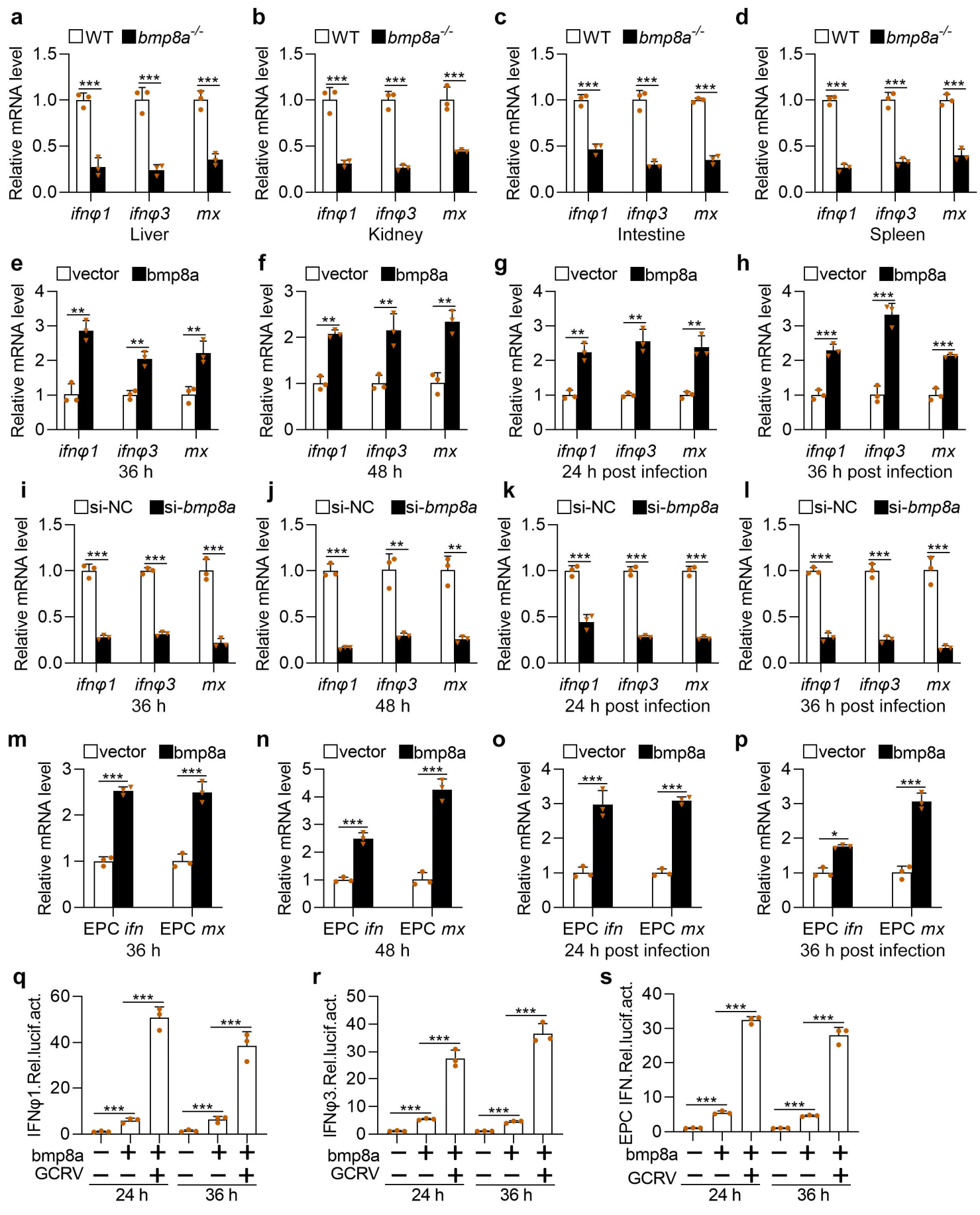

Fig.2 Bmp8a promotes antiviral innate immune responses. a-d Expression of *ifnφ1*, *ifnφ3*, and *mx* mRNA in the liver, kidney, intestine, and spleen from WT or *bmp8a*$^{-/-}$ zebrafish injected i.p. with 50 μl of GCRV (10^8TCID$_{50}$ per ml) for 72 h. **e**, **f** Expression of *ifnφ1*, *ifnφ3*, and *mx* mRNA after transfected with bmp8a (2 μg) or empty vector (2 μg) in ZFL cells. The cells were collected at 36 h (**e**) or 48 h (**f**) post transfection. **g, h** Expression of *ifnφ1*, *ifnφ3*, and *mx* mRNA after transfected with bmp8a (2 μg) or empty vector (2 μg) in ZFL cells for 24 h, followed by infection with GCRV for another 24 h (**g**) or 36 h (**h**). **i**, **l** Expression of *ifnφ1*, *ifnφ3*, and *mx* mRNA after *bmp8a* knockdown in ZFL cells. The cells were collected at 36 h (**i**) or 48 h (**l**) post knockdown. **k**, **l** Expression of *ifnφ1*, *ifnφ3*, and *mx* mRNA after knockdown *bmp8a* in ZFL cells for 24 h, followed by infection with GCRV for another 24h (**k**) or 36 h (**l**). **m**, **n** Expression of EPC *ifn* and EPC *mx* mRNA after transfected with bmp8a (2 μg) or empty vector (2 μg) in EPC cells. The cells were collected at 36 h (**m**) or 48 h (**n**) post

163 transfection. **o**, **p** Expression of EPC *ifn* and EPC *mx* mRNA after transfected with bmp8a (2 μg) or empty vector (2 μg) in
164 EPC cells for 24 h, followed by infection with GCRV for another 24 h (**o**) or 36 h (**p**). The expression of zebrafish *actb1* or
165 EPC *actin* was used as an internal control for the qRT-PCR. **q-s** EPC cells were transfected with IFNφ1pro-luc (200 ng,
166 **q**), IFNφ3pro-luc (200 ng, **r**) or EPC IFN pro-luc (200 ng, **s**) respectively, with or without bmp8a (200 ng), followed by
167 infection with GCRV. At the indicated time points, cells were collected for luciferase assays. *Renilla* luciferase was used
168 as the internal control. Data were from three independent experiments and were analyzed by Student's *t*-test (two-tailed)
169 and were presented as mean ± SD (**$p < 0.01$, ***$p < 0.001$). Source data are provided as a Source Data file.
170
171 **Bmp8a activated Tbk1-Irf3-Ifn antiviral signaling via p38 MAPK pathway.** To putatively examine the molecular mechanism
172 by which Bmp8a stimulates *ifn* and *mx* expression, we carried out transcriptome analysis of the livers of *bmp8a*$^{-/-}$ mutant and
173 wild-type zebrafish, that both had been intraperitoneally injected with GCRV. Kyoto Encyclopedia of Genes and Genomes
174 (KEGG) analyses revealed that, compared with wild-type zebrafish, the down-regulated genes in the mutant were remarkably
175 enriched in the RIG-I-like receptor signaling pathway, NF-kappa B signaling pathway, TNF signaling pathway, and protein
176 digestion and absorption that function in the antiviral immune process (Supplementary Fig. 3). In agreement with transcriptome
177 analysis, we found that the expressions of *tbk1*, *irf3*, and *irf7* were significantly upregulated in bmp8a-overexpressing ZFL cells
178 than control cells, infected with or without GCRV (Fig. 3a-d). Similar expression patterns of *tbk1*, *irf3*, and *irf7* were also observed
179 in EPC cells, infected with or without GCRV (Fig. 3e-h). In addition, *bmp8a* knockdown resulted in considerably reduced
180 expression of *tbk1*, *irf3*, and *irf7* in ZFL cells than control cells, infected with or without GCRV (Fig. 3i-l). We then evaluated the
181 activation of Tbk1 and Irf3 by immunoblot assays in both bmp8a-overexpressing and wild-type ZFL cells as well as EPC cells,
182 infected with or without GCRV. It was found that phosphorylation levels of Tbk1 and Irf3 were significantly increased in both
183 types of the cells with overexpressed Bmp8a (Fig. 3m-p). Moreover, *bmp8a* knockdown markedly reduced the phosphorylation
184 levels of Tbk1 and Irf3 in ZFL cells, infected with or without GCRV (Fig. 3q, r). Furthermore, in luciferase activity assays,
185 transfection of dominant negative mutations of *tbk1* (tbk1-K38M), *irf3* (irf3DN), or *irf7* (irf7DN) in EPC cells induced a significant
186 loss in the ability of Bmp8a to activate the IFN promoter (Fig. 3s-u). This was further supported by the observations *in vivo* that
187 the expression of *tbk1*, *irf3*, and *irf7* in the liver, kidney, intestine, and spleen was significantly downregulated in *bmp8a*$^{-/-}$ mutant
188 than that in wild-type zebrafish (Fig. 3v-y). These data together revealed that Bmp8a induced *ifn* and *mx* expression via
189 promoting Tbk1-Irf3-Ifn antiviral signaling.
190 BMPs transmit signals through smad1/5/8, smad2/3, ERK, JNK, or p38 MAPK pathways[39-41]. Thus, the effects of p38
191 MAPK inhibitor SB203580, JNK inhibitor SP600125, MEK1/2 inhibitor U0126, SMAD1/5/8 inhibitor DMH1, and smad2/3
192 inhibitor TP0427736 HCl on the expression of *ifn* was tested in bmp8a-overexpressing ZFL cells and EPC cells. We have
193 shown above that Bmp8a overexpression increased the expression of *ifn* (Fig. 2). Here we found that only p38 MAPK

194 inhibitor SB203580 significantly reduced the expression of *ifnφ1* and *ifnφ3* in ZFL cells and the expression of *ifn* in EPC
195 cells (Fig. 4a-c). Furthermore, the IFN promoter-driven luciferase assays revealed that the luciferase activities were
196 markedly reduced in EPC cells upon treatment with p38 MAPK inhibitor SB203580 (Fig. 4d-f), consistent with the
197 observation that Bmp8a induced the expression of *ifn* through p38 MAPK pathway. Taken the previous report that the
198 MAPK signaling increased the phosphorylation of TBK1 and IRF3 upon viral infection into consideration[42], we suggested
199 that Bmp8a activated Tbk1-Irf3-Ifn antiviral signaling via p38 MAPK pathway.

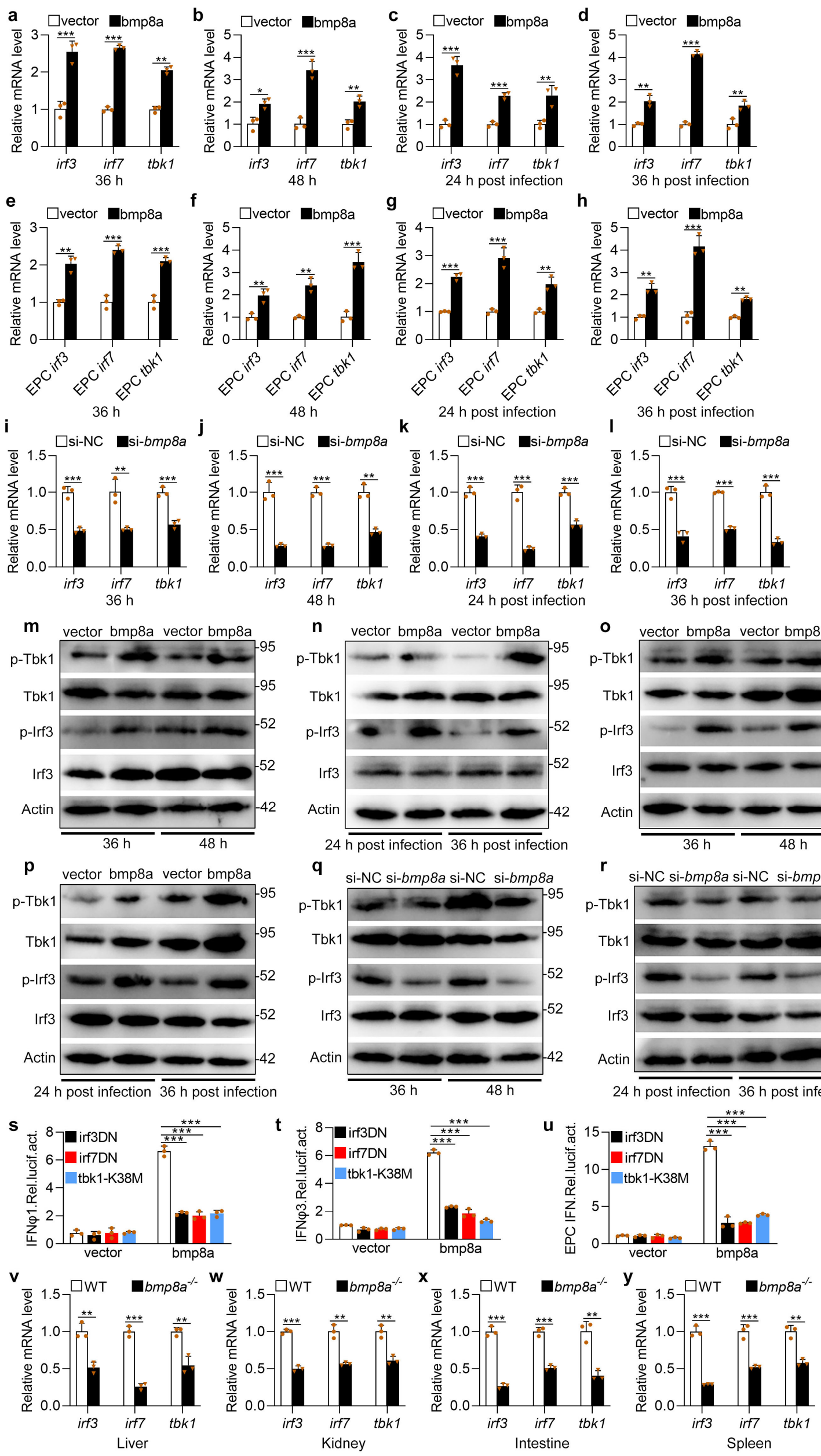
a
vector
bmp8a
Relative mRNA level
irf3
irf7
tbk1
36 h
b
48 h
c
24 h post infection
d
36 h post infection
e
EPC irf3
EPC irf7
EPC tbk1
f
g
h
i
si-NC
si-bmp8a
j
k
l
m
vector bmp8a vector bmp8a
p-Tbk1
Tbk1
p-Irf3
Irf3
Actin
n
o
p
q
si-NC si-bmp8a si-NC si-bmp8a
r
s
IFNφ1.Rel.lucif.act.
irf3DN
irf7DN
tbk1-K38M
t
IFNφ3.Rel.lucif.act.
u
EPC IFN.Rel.lucif.act.
v
WT
bmp8a-/-
Liver
w
Kidney
x
Intestine
y
Spleen

201 **Fig.3 Bmp8a increases Tbk1-Irf3-Ifn antiviral signaling. a**, **b**, **e**, **f** Expression of *irf3*, *irf7*, and *tbk1* mRNA after
202 transfected with 2 μg bmp8a or empty vector in ZFL (**a**, **b)** or EPC (**e**, **f)** cells. The cells were collected at 36 h (**a**, **e**) or 48
203 h (**b**, **f**) post transfection. **c**, **d**, **g**, **h** Expression of *irf3*, *irf7*, and *tbk1* mRNA after transfected with 2 μg bmp8a or empty
204 vector in ZFL (**c**, **d)** or EPC **(g**, **h)** cells for 24 h, followed by infection with GCRV for another 24 h (**c**, **g**) or 36 h (**d**, **h**). **i, j,**
205 **k, l** Expression of *irf3*, *irf7*, and *tbk1* mRNA after *bmp8a* knockdown in ZFL cells. The cells were collected at 36 h (**i**) and
206 48 h (**j**) post knockdown or at 24 h (**k**) and 36 h (**l**) post infected with GCRV. **m**, **o** Immunoblot analysis of phosphorylated
207 (p-) Tbk1 and Irf3 after transfected with 2 μg bmp8a or empty vector in ZFL (**m**) or EPC (**o**) cells. The cells were collected
208 at 36 h or 48 h post transfection for Immunoblot analysis. **n**, **p** Immunoblot analysis of phosphorylated (p-) Tbk1 and Irf3
209 after transfected with 2 μg bmp8a or empty vector in ZFL (**n**) or EPC (**p**) cells for 24 h, followed by infection with GCRV
210 for another 24 h or 36 h. **q**, **r** Immunoblot analysis of phosphorylated (p-) TBK1 and IRF3 after *bmp8a* knockdown in ZFL
211 cells. The cells were collected at 36 h and 48 h post knockdown or at 24 h and 36 h post infected with GCRV. **s-u** EPC
212 cells were cotransfected with IFN-φ1pro-luc (200 ng, **s**), IFN-φ3pro-luc (200 ng, **t**) or EPC IFNpro-luc (200ng, **u**), and
213 bmp8a (100 ng) together with each of the dominant negative plasmids including tbk1-K38M (100 ng), irf3DN (100 ng) and
214 irf7DN (100 ng). At 48 h post transfection, the cells were collected for luciferase assays. *Renilla* luciferase was used as
215 the internal control. **v-y** Expression of *irf3*, *irf7*, and *tbk1* mRNA in the liver, kidney, intestine, and spleen from WT or *bmp8a*$^{-}$
216 $^{/-}$ zebrafish injected i.p. with 50 μl of GCRV (10^8TCID$_{50}$ per ml). The expression of zebrafish *actb1* or EPC *actin* was used
217 as an internal control for the qRT-PCR. Data were from three independent experiments and were analyzed by Student's
218 *t*-test (two-tailed) and were presented as mean ± SD (***p* < 0.01, ****p* < 0.001). Source data are provided as a Source
219 Data file.

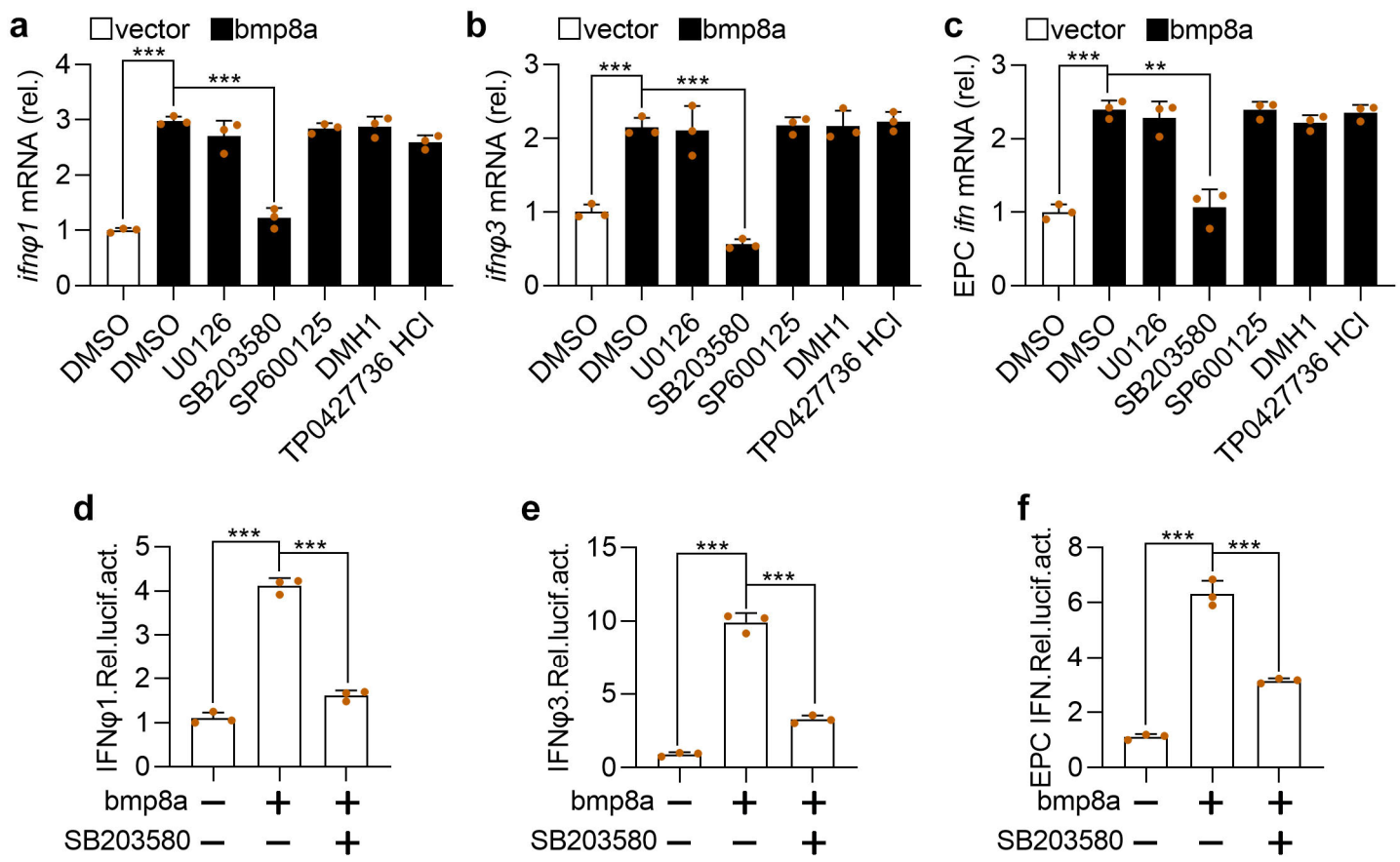

Fig.4 Bmp8a promotes the IFN expression via p38 MAPK pathway. a, **b** Expression of *ifnφ1* (**a**) and *ifnφ3* (**b**) mRNA after transfected with bmp8a (2 μg) in ZFL cells for 24 h, followed by treatment with SB203580, SP600125, U0126, DMH1 and TP0427736 HCl for another 24 h. **c** similar as (**a**, **b**) but in EPC cells. The expression of zebrafish *actb1* or EPC *actin* was used as an internal control for the qRT-PCR. **d-f** EPC cells were cotransfected with IFNφ1pro-luc (200 ng, **d**), IFNφ3pro-luc (200 ng, **e**) or EPC IFNpro-luc (200 ng, **f**), pRL-TK (20 ng) together with bmp8a (200 ng) or empty vector (200 ng), respectively. At 24 h post transfection, cells were treated with or without SB203580 for another 24 h and then harvested for detection of luciferase activity. *Renilla* luciferase was used as the internal control. Data were from three independent experiments and were analyzed by Student's *t*-test (two-tailed) and were presented as mean ± SD (**$p < 0.01$, ***$p < 0.001$). Source data are provided as a Source Data file.

BMP type I receptor Alk6a interacted with Bmp8a and participated in antiviral immunity. BMPs exert their biological effects through the sequential activation of two types of transmembrane receptors, namely BMP receptor type I and BMP receptor type II, that both possess intrinsic serine/threonine kinase activity[43,44]. To detect which receptor is involved in the regulation of the antiviral immune responses, the expression of both type I receptor genes (*alk2*, *alk3*, *alk6a*) and type II receptor genes (*bmpr2a*, *bmpr2b*, *actr2a*, *actr2b*) in ZFL cells transfected with poly(I:C) or infected with GCRV were measured. Among these receptor genes, *alk6a* showed the highest expression upon poly(I:C) or virus challenge (Fig. 5a, b). We also overexpressed all these receptors in ZFL and EPC cells, and examined the expression of *ifn* in these cells. The upregulation of *ifnφ1* was only found in the alk6a-overexpressing ZFL cells (Fig. 5c). Moreover, the overexpression of *alk6a* or *alk2* resulted in significantly increased expression of *ifnφ3* in ZFL cells and *ifn* in EPC cells, with overexpressed

240 *alk6a* being more effective (Fig. 5d, e). Based on these findings, the function of Alk6a was selected for further test.
241 Compared to wild-type ZFL cells, the expressions of antiviral protein genes *ifnφ1, ifnφ3* and *mx* as well as the antiviral
242 signaling genes *tbk1*, *irf3*, and *irf7* were all markedly upregulated in alk6a-overexpressed ZFL cells with or without GCRV
243 infection (Fig. 5f, g). The similar results were also observed in the alk6a-overexpressed EPC cells (Fig. 5h, i). Because
244 the phosphorylation of Gly-Ser (GS) domain of the type I receptor is required for its activation, we thus constructed
245 dominant-negative mutant of alk6a (alk6a-ΔGS) plasmid (Fig. 5j), and then transferred it into both ZFL and EPC cells. It
246 revealed that the dominant-negative mutation of *alk6a* significantly reduced the expression of *mx, ifn* (*ifnφ1* and *ifnφ3* in
247 ZFL cells), *tbk1*, *irf3*, and *irf7* in ZFL and EPC cells, with or without GCRV infection (Fig. 5k-n). The data suggested that
248 Alk6a was apparently involved in the Tbk1-Irf3/7-Ifn antiviral signaling.

249 Considering we have revealed that Bmp8a activated Tbk1-Irf3-Ifn antiviral signaling via p38 MAPK pathway, we then
250 examined whether the the levels of phosphorylated p38 MAPK protein were regulated by Alk6a. Clearly, compared to wild-
251 type ZFL or EPC cells, phosphorylation levels of p38 MAPK were significantly increased in alk6a-overexpressed both
252 types of the cells with or without GCRV infection (Fig. 6a-d). Moreover, dominant-negative mutation of *alk6a* significantly
253 reduced the phosphorylation levels of p38 MAPK in ZFL or EPC cells, with or without GCRV infection (Fig. 6e-h). Thus,
254 Alk6a was shown to be involved in the phosphorylation of p38 MAPK. Next, we investigated whether the antiviral immune
255 responses of Bmp8a were mediated by Alk6a. In the IFN promoter-driven luciferase assays, it was found that the ability
256 of Bmp8a to activate the IFN promoter was markedly blocked after the dominant-negative mutation of *alk6a* in EPC cells
257 (Fig. 6i-k). Importantly, co-immunoprecipitation (Co-IP) experiments confirmed that Bmp8a interacted with Alk6a (Fig. 6l).
258 Collectively, our data demonstrated that BMP type I receptor Alk6a interacted with Bmp8a, and participated in the antiviral
259 immunity. To our best knowledge, Alk6a is the first BMP receptor identified thus far which is being directly required for
260 antiviral immune responses.

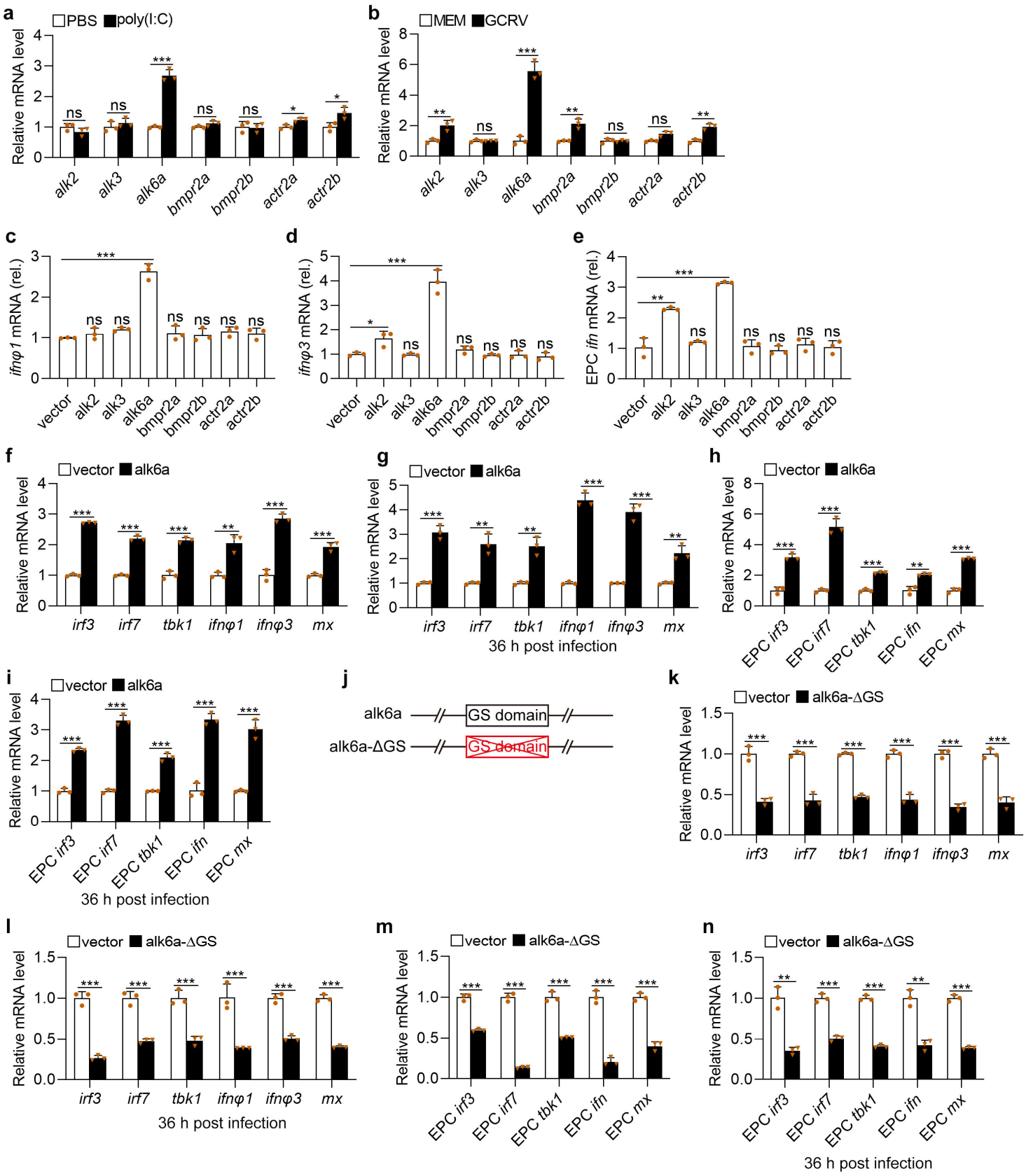

Fig. 5 Alk6a is involved in the antiviral innate immune responses. a, **b** Expression of *alk2*, *alk3*, *alk6a*, *bmpr2a*, *bmpr2b*, *actr2a*, *actr2b* mRNA in ZFL cells stimulated with GCRV (5 × 10^4TCID$_{50}$ per ml, **a**) or poly(I:C) (2 μg/ml, **b**) for 48 h. **c-e** Expression of *ifnφ1* (**c**) and *ifnφ3* (**d**) mRNA in ZFL cells or EPC *ifn* (**e**) in EPC cells which were transfected with 2 μg of alk2, alk3, alk6a, bmpr2a, bmpr2b, actr2a, actr2b or empty vector for 48 h. **f, h** Expression of *irf3*, *irf7*, *tbk1*, *ifn* (or *ifnφ1* and *ifnφ3*), and *mx* mRNA after transfected with 2 μg of pcDNA3.1-alk6a or empty vector in ZFL (**f**) or EPC (**h**) cells for 48 h. **g, i** Expression of *irf3*, *irf7*, *tbk1*, *ifn* (or *ifnφ1* and *ifnφ3*), and *mx* mRNA after transfected with 2 μg of of pcDNA3.1-alk6a or empty vector in ZFL (**g**) or EPC (**i**) cells for 24 h, followed by infection with GCRV for another 36 h. **j** Schematic drawing of the alk6a-ΔGS mutation that the GS domain of Alk6a was deleted. **k, m** Expression of *irf3*, *irf7*, *tbk1*, *ifn* (or *ifnφ1* and *ifnφ3*), and *mx* mRNA after transfected with 2 μg pcDNA3.1-alk6a-ΔGS or empty vector in ZFL (**k**) or EPC (**m**) cells for 48 h. **l, n** Expression of *irf3*, *irf7*, *tbk1*, *ifn* (or *ifnφ1* and *ifnφ3*), and *mx* mRNA after transfected with 2 μg pcDNA3.1-

alk6a-ΔGS or empty vector in ZFL (**l**) or EPC (**n**) cells for 24 h, followed by infection with GCRV for another 36 h. The expression of zebrafish *actb1* or EPC *actin* was used as an internal control for the qRT-PCR. Data were from three independent experiments and were analyzed by Student's *t*-test (two-tailed) and were presented as mean ± SD (*$p < 0.05$, **$p < 0.01$, *** $p < 0.001$, ns means no significant difference). Source data are provided as a Source Data file.

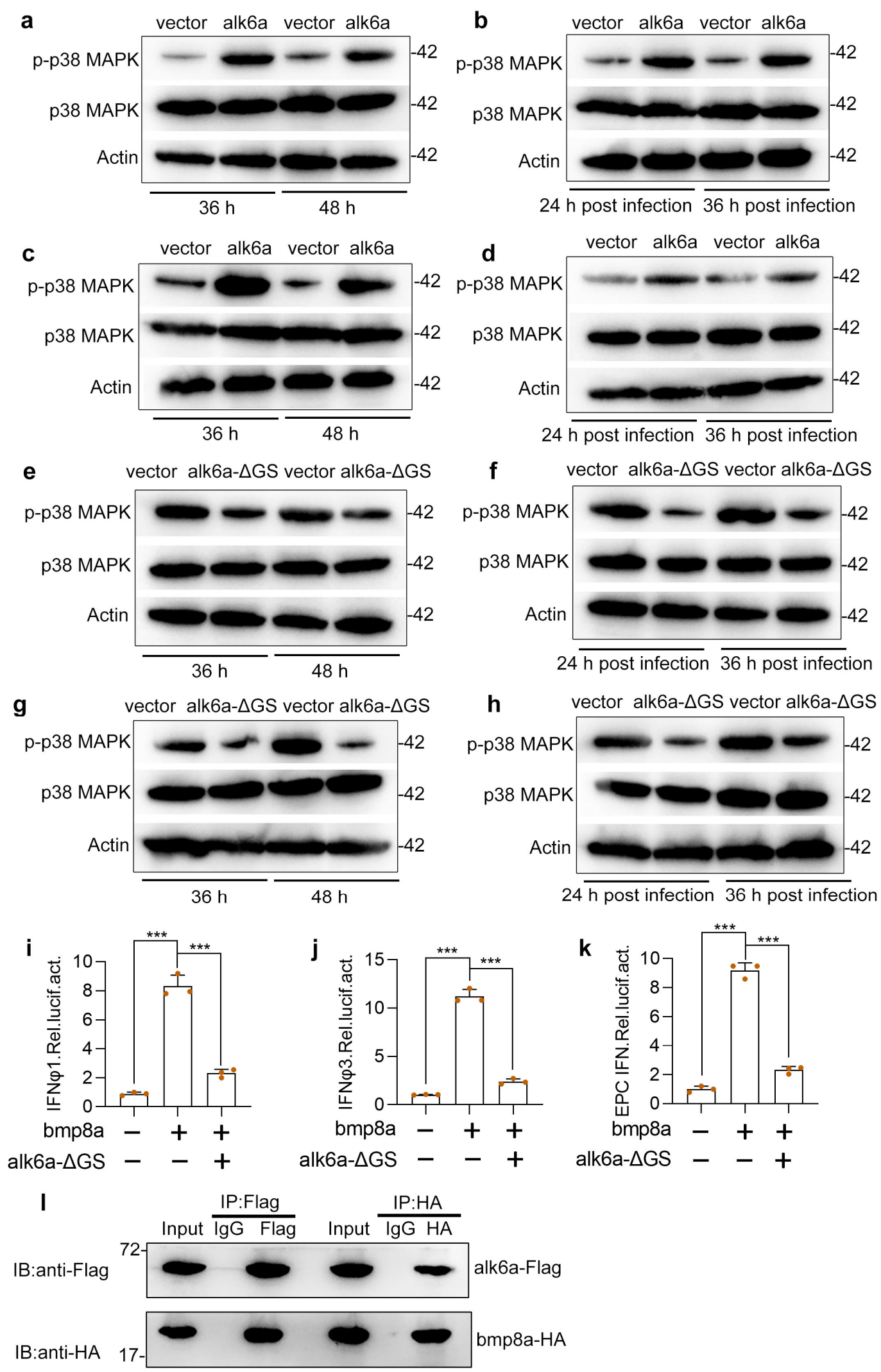

Fig. 6 Bmp8a activates the IFN expression through Alk6a. a, **c** Immunoblot analysis of phosphorylated (p-) p38 MAPK after transfected with 2 μg alk6a or empty vector in ZFL (**a**) or EPC (**c**) cells. The cells were collected at 36 h or 48 h post transfection for Immunoblot analysis. **b**, **d** Immunoblot analysis of phosphorylated (p-) p38 MAPK after transfected with 2 μg alk6a or empty vector in ZFL (**b**) or EPC (**d**) cells for 24 h, followed by infection with GCRV ($5 \times 10^4 TCID_{50}$ per ml) for

281 another 24 h or 36 h. **e, g** Immunoblot analysis of phosphorylated (p-) p38 MAPK after transfected with 2 μg alk6a-ΔGS
282 or empty vector in ZFL (**e**) or EPC (**g**) cells. The cells were collected at 36 h or 48 h post transfection for Immunoblot
283 analysis. **f**, **h** Immunoblot analysis of phosphorylated (p-) p38 MAPK after transfected with 2 μg alk6a or empty vector in
284 ZFL (**f**) or EPC (**h**) cells for 24 h, followed by infection with GCRV ($5 \times 10^4 TCID_{50}$ per ml) for another 24 h or 36 h. **i-k** EPC
285 cells were cotransfected with IFN-φ1pro-luc (200 ng, **i**), IFN-φ3pro-luc (200 ng, **j**) or EPC IFNpro-luc (200ng, **k**), and
286 bmp8a (100 ng) together with or without the dominant negative plasmids alk6a-ΔGS (100 ng). At 48 h post transfection,
287 the cells were collected for luciferase assays. *Renilla* luciferase was used as the internal control. **l** Co-immunoprecipitation
288 and immunoblot analysis of EPC cells cotransfected with alk6a-Flag (1 μg) and bmp8a-HA (1μg). Data were from three
289 independent experiments and were analyzed by Student's *t*-test (two-tailed) and were presented as mean ± SD (*** $p<$
290 0.001). Source data are provided as a Source Data file.
291
292 **Virus induced expression of *bmp8a*.** Next, we measured the expression of *bmp8a* in ZFL cells upon virus infection.
293 GCRV significantly induced the expression of *bmp8a* at 12 h post-stimulation, and reached a peak at 48 h (Fig. 7a). We
294 also detected the expression of *bmp8a* upon infection with GCRV or poly(I:C) *in vivo*. The expression of *bmp8a* in the liver,
295 kidney, intestine, and spleen of zebrafish infected with GCRV or poly(I:C) was all significantly elevated (Fig. 7b-i). This
296 indicated that the expression of *bmp8a* was inducible by infection with virus or its mimic poly(I:C).

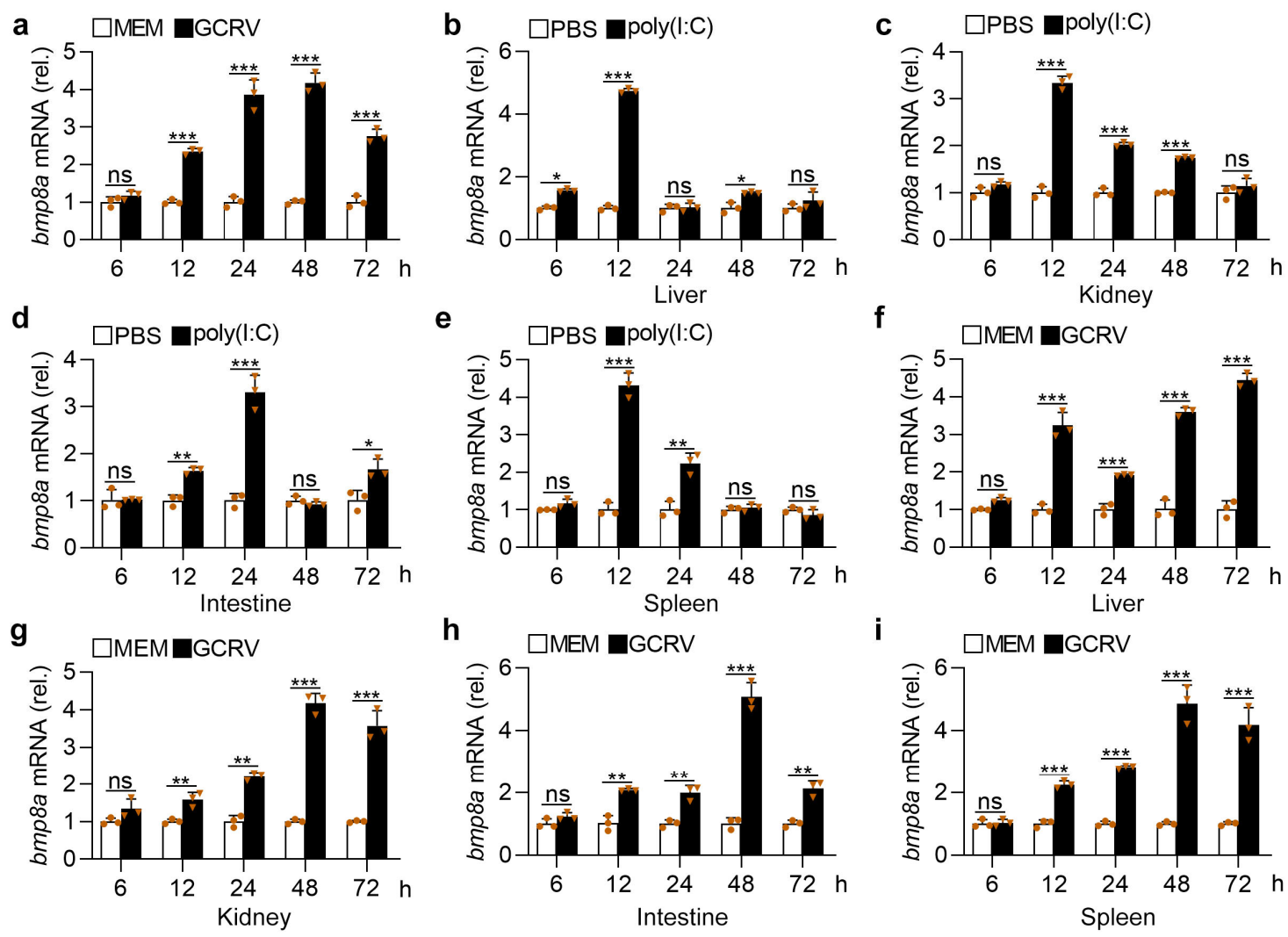

297
298 **Fig. 7 GCRV or poly(I:C) increases the expression of *bmp8a*. a** Expression of *bmp8a* mRNA in ZFL cells after infected

299 with GCRV (5 × 10^4TCID$_{50}$ per ml) for 48 h. **b-e** Expression of *bmp8a* mRNA in the liver (**b**), spleen (**c**), intestine (**d**), and
300 kidney (**e**) from zebrafish injected i.p. with poly(I:C) (10 μg/fish). **f-i** Expression of *bmp8a* mRNA in the liver (**f**), spleen (**g**),
301 intestine (**h**), and kidney (**i**) from zebrafish injected i.p. with 50μl of GCRV (10^8TCID$_{50}$ per ml). Zebrafish injected i.p. with
302 PBS or MEM were used as the control. The expression of *actb1* served as a control for the qRT-PCR. Data were from
303 three independent experiments and were analyzed by Student's *t*-test (two-tailed) and were presented as mean ± SD (*p
304 < 0.05, **p < 0.01, ***p < 0.001, ns means no significant difference). Source data are provided as a Source Data file.
305

306 **Binding of Stat1 to GAS motifs activated *bmp8a* expression.** To explore how virus induces expression of *bmp8a*, we
307 searched for the transcription factor binding sites in *bmp8a* promoter region at the web http://jaspar.genereg.net/. Two
308 gamma-activated sites (GAS), 5'-ATTCCGGGAAA-3' (P1) and 5'-TTTACTAGAAC-3' (P2), in *bmp8a* promoter region were
309 identified (Supplementary Fig. 4). In mammals, the transcription factor STAT1 homodimer was known to bind to the GAS
310 motif in the promoter region of IFN-γ triggered downstream genes[11,16]. We thus wonder if Stat1 can bind to the *bmp8a*
311 promoter region to activate the expression of *bmp8a*. In zebrafish, there exist two Stat1 factors, Stat1a (GenBank
312 accession number NM_131480.1) and Stat1b (GenBank accession number NM_200091.2). Thus we constructed
313 dominant-negative mutant plasmids of stat1a-ΔC and stat1b-ΔC, that were transferred into ZFL cells, respectively. It was
314 found that the expression of *bmp8a* was significantly blocked in both cases (Fig. 8a, b). By contrast, the overexpression
315 of either *stat1a* or *stat1b* markedly promoted *bmp8a* promoter-driven luciferase activities (Fig. 8c). In addition, when one
316 of the GAS motifs in *bmp8a* promoter region was deleted, *bmp8a* promoter-driven luciferase activities were significantly
317 reduced; when both of the GAS motifs were deleted, *bmp8a* promoter-driven luciferase activities were reduced even more
318 significantly (Fig. 8d, e). These suggested that both Stat1a and Stat1b may interact with the GAS motifs.

319 To verity the binding of Stat1a/Stat1b to the GAS motifs in *bmp8a* promoter region, the recombinant proteins of both
320 Stat1a and Stat1b were expressed and purified (Fig. 8f, g), and used for electrophoretic mobility shift assay (EMSA). As
321 shown in Fig. 8h-k, a remarkable band of protein-DNA complex was observed (lane 2). The protein-DNA complex band
322 was obviously weaker in the presence of an excess unlabeled competitor probe, compared to that of biotin labeled probe
323 group (lane 3), but the intensity of the band showed little change in the presence of GAS mutant probes (lane 4). To detect
324 the specific binding, a supershift experiment with the antibody against His tag was performed. It revealed that His tag
325 antibody caused a specific supershift of slower migrating protein-DNA-antibody complex (Fig. 8h-k, lane 5). There was no
326 protein-DNA complex observed in the negative control group (Fig. 8h-k, lane 1). These demonstrated that both Stat1a and
327 Stat1b could directly bind to the GAS motifs in *bmp8a* promoter region, suggesting that *bmp8a* expression was subjected
328 to the regulation by binding of Stat1a/Stat1b to the GAS motifs.

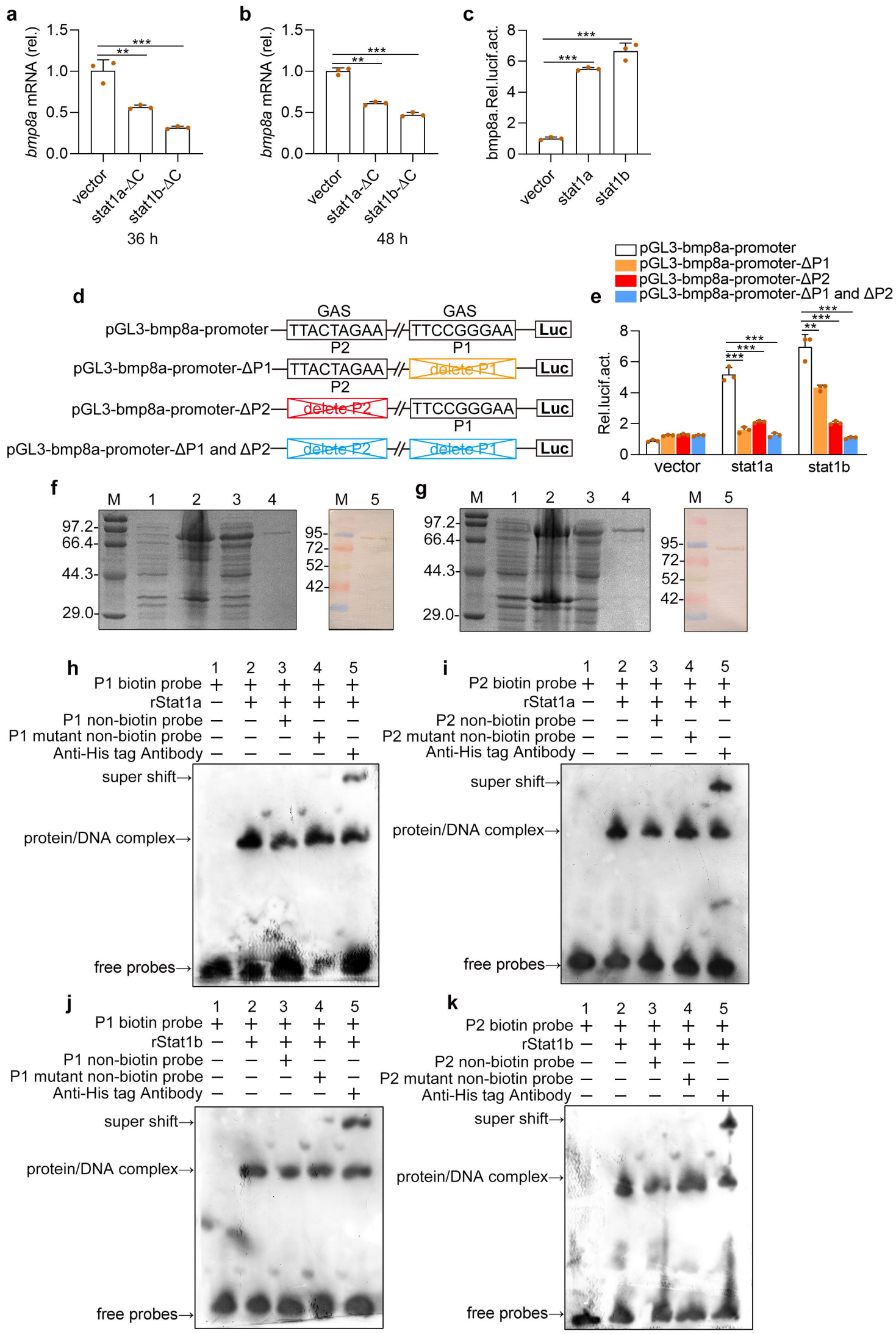

Fig. 8 Stat1 binds the GAS sites and activates the *bmp8a* transcriptions upon virus stimulation. a, b Expression of *bmp8a* mRNA in ZFL cells after transfected with stat1a-ΔC or stat1b-ΔC for 36 h (**a**) or 48 h (**b**). The expression of *actb1* served as a control for the qRT-PCR. **c** Dual luciferase report assay was used to analyze the transcription abilities of

333 Stat1a and Stat1b in activation of *bmp8a* in EPC cells. pGl3-bmp8a (200 ng) was transfected into EPC cells together with
334 stat1a (200 ng), stat1b (200 ng) or empty vector (200 ng). After 48 h, the transfected cells were collected for luciferase
335 assays. **d** Schematic drawing of wild-type and GAS motif mutation Luc-report plasmids. **e** The 200 ng of pGL3-bmp8a-
336 promoter, pGL3-bmp8a-promoter-ΔP1, pGL3-bmp8a-promoter-ΔP2 or pGL3-bmp8a-promoter-ΔP1 and ΔP2 was
337 transfected into EPC cells along with stat1a (200 ng), stat1b (200 ng) or empty vector (200 ng), respectively. After 48 h,
338 the transfected cells were collected for luciferase assays. *Renilla* luciferase was used as the internal control. **f**, **g** SDS-
339 PAGE and Western-blotting analysis of rStat1a (**f**) and rStat1b (**g**). Lane M: protein molecular standard; Lane 1: negative
340 control for IPTG induced *E. coli* (without rStat1a or rStat1b); Lane2: induced rStat1a or rStat1b (the whole cell lysate);
341 Lane 3: induced rStat1a or rStat1b (the supernatant); Lane 4: purified rStat1a or rStat1b; Lane 5: western blot analysis of
342 the sample in Lane 4. **h-k** EMSA was performed to validate the interaction of rStat1a or rStat1b with the GAS motif (P1 or
343 P2) in the bmp8a promoter region. Lane 1: negative group; Lane 2: positive group; Lane 3: an excess unlabeled competitor
344 probe; Lane 4: an excess unlabeled competitor probe containing a mutated runt binding site; Lane 5: Super-shift assays
345 were performed by adding antibody against His tag. Data were from three independent experiments (**a–c, e**) or two
346 independent experiments (**f-k**). Data were analyzed by Student's *t*-test (two-tailed) and were presented as mean ± SD (**$p < 0.01$,***$p < 0.001$). Source data are provided as a Source Data file.
347
348

349 **Discussion**

350 BMPs, canonical multi-functional growth factors, are suggested to play roles in regulation of immune responses, but
351 it remains controversial over their functions in immunity. We show here for the first time that Bmp8a is a previously
352 unrecognized factor involved in the regulation of antiviral immune responses in zebrafish. Evidences supporting this nature
353 of Bmp8a include: Bmp8a inhibits RNA viruses replication *in vitro* and *in vivo*; Bmp8a promotes the expression of antiviral
354 protein genes including type I IFNs and *mx*; the expression of *bmp8a* is induced by CGRV or poly(I:C), and Bmp8a activates
355 TBK1-IRF3-IFN signaling. Bmp8a is a member of the TGF-β superfamily, which includes more than 30 genes encoding
356 TGFβ, BMPs and activins. TGFβ has been shown to have both pro- and anti-inflammatory effects depending on the
357 context it is acting in the immune system[45]. Like TGFβ, BMP members have also been shown to play different
358 immunoregulatory roles[46]. BMP2, 4 and 7 deficiency or knockdown results in partial loss of the thymic capsule, reduced
359 size of thymus and increased *Helicobacter pylori*-induced inflammation, whereas BMP6 inhibits macrophage growth by
360 inducing cell cycle arrest *in vitro*[27,47-50]. The finding that Bmp8a is a positive regulator in antiviral immune responses
361 provides a new angle for our understanding of the functions of TGF-β superfamily members including BMPs.

362 On one hand, it is generally regarded that the recognition of virus by PRRs elicits the activation of IRF3 and NF-κB,
363 and induces the production of IFNα/β, that then activate JAK-STAT pathway, eventually leading to the production of ISGs

364 such as cytokines and antiviral proteins. On the other hand, BMPs are known to transmit signals through both Smad-
365 dependent pathways (smad1/5/8 and smad2/3 pathways) and Smad-independent pathways (ERK, JNK, and p38 MAPK
366 pathways). Here we clearly demonstrate that Bmp8a promotes the expression of endogenous type I IFNs independent of
367 Smad signaling pathways. Moreover, it is p38 MAPK pathway, rather than ERK and JNK pathways, that is involved in the
368 antiviral responses induced by Bmp8a. Furthermore, we show that Alk6a participates in Tbk1-Irf3/7-Ifn antiviral signaling
369 via interaction with Bmp8a. In addition, Alk6a was found to be required to induce the phosphorylation of p38 MAPK, which
370 is consistent with the findings in mouse that Alk6 knockdown suppresses p38 MAPK phosphorylation[51]. Previous studies
371 have shown that MAPK signaling pathway is crucial in the phosphorylation of TBK1 and IRF3 upon viral infection[42]. Thus,
372 we probably discover a new pathway of Bmp8a signaling in antiviral immune responses that Bmp8a acts as a positive
373 regulator through the promotion of phosphorylation of Tbk1 via p38 MAPK pathway, i.e., Bmp8a binds to Alk6a, which
374 induces p38 MAPK phosphorylation, and in turn enhances Tbk1 and Irf3 phosphorylation, eventually resulting in increased
375 synthesis of type I IFN (Fig. 9).

376 Our study also show that the challenge with GCRV and poly(I:C) both significantly promotes the expression of
377 zebrafish *bmp8a*. Searching for the binding sites of transcript factors in *bmp8a* promoter region reveals that two IFN-γ
378 activation sites (GAS) that may interact with STAT1 are identified. Functionally, we demonstrate that Stat1a and Stat1b,
379 orthologues of human STAT1, can directly bind the GAS sites in *bmp8a* promoter, resulting in activation of *bmp8a*
380 expression. It has been reported that in black carp, Stat1a and Stat1b can both form homodimer and heterodimer *in vivo*
381 like their mammalian counterpart[52]. It is thus highly likely that in zebrafish, Stat1a and Stat1b can form homodimer or
382 heterodimer, which then binds to the GAS sites in *bmp8a* promoter region. In zebrafish, IFN-γ has been found to be able
383 to induce the expression of both *stat1a* and *stat1b*, and the GAS motif is required for Ifn-γ activation[53,54]. It is widely known
384 that the JAK-STAT pathway is one of the most important candidate pathways through which IFN-γ works. Activation of
385 JAK-STAT signaling leads to transcription of various downstream ISGs for antiviral activity[55]. We thus think that Bmp8a is
386 another important antiviral factor which can be activated through Ifn-γ-Jak-Stat1 pathway (Fig. 9).

387 In summary, we demonstrate for the first time that Bmp8a is a positive regulator in antiviral immune responses, which
388 functions through promotion of phosphorylation of Tbk1 via p38 MAPK pathway. Upon virus infection, the expression of
389 *bmp8a* is activated by Stat1a/Stat1b directly. Bmp8a knockdown leads to significantly decreased phosphorylation of Tbk1
390 and Irf3. As a consequence, *bmp8a*-deficient zebrafish produces significantly lowered type I IFNs in response to RNA
391 virus infection, exhibits significantly reduced immune responses, and increases significantly higher viral load and morbidity
392 *in vivo*. Our study is significant to understand the regulatory mechanism of BMP involving in antiviral immune response
393 and provides a new target for controlling viral infection.

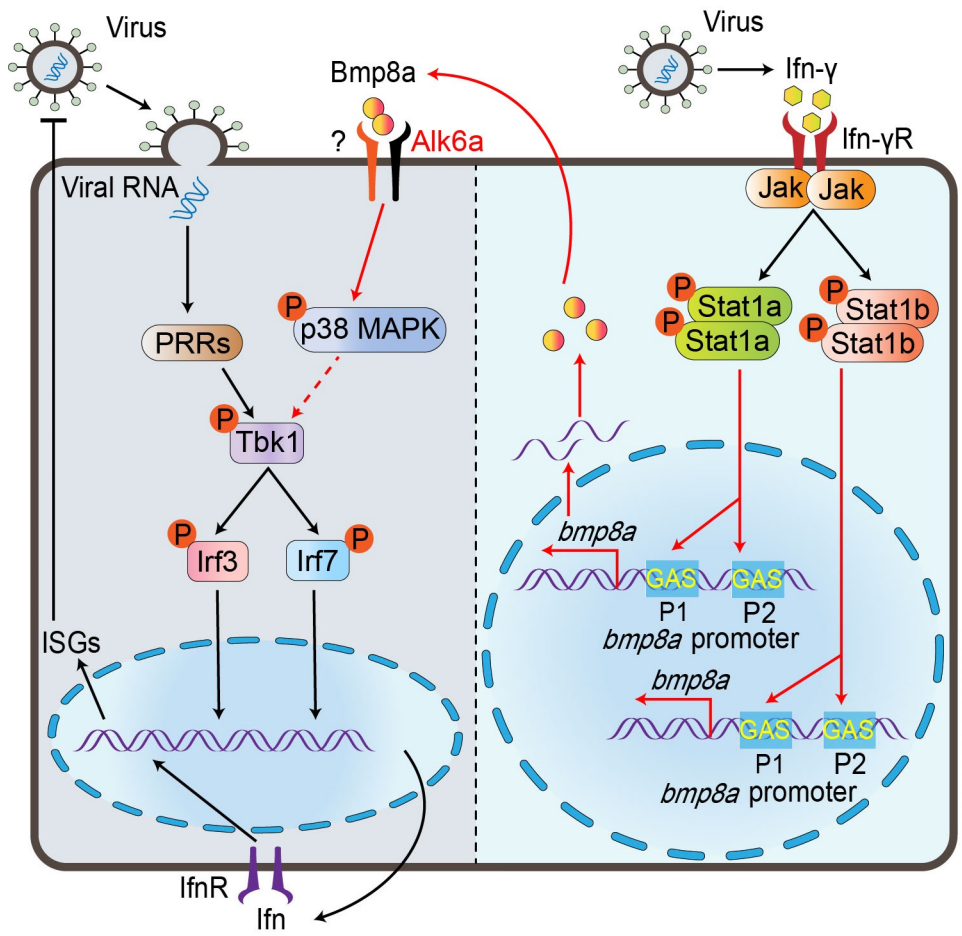

Fig. 9 Schematic illustration of Bmp8a serving as positive regulator in the antiviral immune. Upon virus infection, the transcriptions of *bmp8a* are activated through the Jak-Stat1 pathway. The Bmp8a binds to BMP type I receptor Alk6a, promoting phosphorylation of Tbk1 and Irf3 to induce the expression of *Ifn* through p38 MAPK pathway.

Methods

Cells and viruses. The epithelioma papulosum cyprini cells (EPC), zebrafish liver cells (ZFL) were acquired from the China Zebrafish Resource Center (CZRC) and cultured according to the instructions from the CZRC. EPC and ZFL cells were grown in a 28 °C incubator supplied with 5% CO_2. The flounder gill cells (FG) were grown in a 22 °C incubator supplied. The EPC or FG cells were cultured in MEM media supplemented with 10% fetal bovine serum (FBS) (Gibco), 100 U/ml penicillin and 100 μg/ml streptomycin. The ZFL cells were maintained in DMEM/F-12 media supplemented with 10% FBS, 100 U/ml penicillin and 100 μg/ml streptomycin. Grass carp reovirus (GCRV), a dsRNA virus, and spring viremia of carp virus (SVCV), a negative ssRNA virus, were kindly provided by Yibing Zhang (Institute of Hydrobiology, Chinese Academy of Sciences), and tittered according to the method of Reed and Muench[56], by a 50% tissue culture infective dose ($TCID_{50}$) assay on EPC cells. The turbot skin verruca disease virus (TSVDV) was isolated from the focal site of turbot skin in our lab.

Zebrafish. The animals used in the experiment followed the ethical guidelines established by the Institutional Animal Care and Use Committee of the Ocean University of China (permit number, SD2007695). The zebrafish *bmp8a* knockout mutant lines (*bmp8a*$^{-/-}$) were established from the zebrafish AB line using TALENs technology. The TALENs for zebrafish *bmp8a*

414 were assembled using the Unit Assembly (UA) method as previously described[57]. All the UA method starting vectors were
415 the gifts from laboratories of Bo Zhang at Peking University and of Shuo Lin at University of California Los Angeles.
416 TALENs mRNAs were transcribed using the mMESSAGE mMACHINE SP6 kit (Invitrogen, #AM1340) and purifified using
417 the RNeasy Mini kit (QIAGEN, #74106). To generate zebrafish mutant lines, TALEN mRNAs (50–200 pg) were
418 microinjected into 1-cell stage zebrafish embryos. Two days after injection, genomic DNA was isolated from 8 to 10 pooled
419 larvae. The target genomic regions were amplified by nested PCR and subcloned into the pGEM-T vector. Single colonies
420 were genotyped by sequencing. To obtain germline mutations, the TALEN-injected embryos were raised to adulthood and
421 outcrossed with wild-type (WT) fish. The F1 progeny were genotyped by sequencing. To obtain homozygous mutants,
422 heterozygous mutant of the same mutation were obtained and self-crossed. The primers used in this study were listed in
423 Supplemental Table 1.
424
425 **Plasmid construction.** The open reading frames (ORF) of zebrafish bmp8a, stat1a, stat1b, alk2, alk3, alk6a, actr2a,
426 actr2b, bmpr2a and bmpr2b were cloned into the pcDNA3.1 expression vector for the eukaryotic expression. The ORF of
427 zebrafish stat1a and stat1b were cloned into the pET-28a expression vector for the expression of recombinant proteins.
428 The promoter regions of bmp8a, bmp8a-ΔP1 (delete the GAS motif of 5´-attccgggaaa-3´ in the bmp8a promoter), bmp8a-
429 ΔP2 (delete another GAS motif of 5´-tttactagaac-3´ in the bmp8a promoter), bmp8a-ΔP1and ΔP2 (delete both the two
430 GAS motifs), IFNφ1, IFNφ3, and EPC IFN were cloned into the pGL3-basic vector. Dominant negative mutant plasmids
431 including tbk1-K38M, stat1a-ΔC, stat1b-ΔC, irf3DN, and irf7DN were described previously[58,59]. Dominant negative mutant
432 plasmids alk6a-ΔGS (delete the sequence of 5´-agctccggttctggctcagga-3´ encoding the GS domain) was cloned into the
433 pcDNA3.1 expression vector. The deletions and mutations were created using Mut Express II Fast Mutagenesis Kit V2
434 (Vazyme, #C214-01). The primers used in this study were listed in Supplemental Table 2.
435
436 **Transcriptome Sequencing.** The zebrafish were fasted for 24 h prior to tissue collection. Three mutant (*bmp8a*$^{-/-}$) and
437 three wild type (WT) adult zebrafish (0.4 g ± 0.05 g) were randomly selected from each group and were injected
438 intraperitoneally with 50 μl of GCRV (10^8TCID$_{50}$ per ml) per fish. Seventy-two hours after the injection, the livers from three
439 fish each group were pooled together for total RNA extraction. Three independent samples from each group were prepared
440 for transcriptome sequencing. mRNAs were enriched by magnetic beads combining the oligo (dT). cDNA fragments were
441 subjected to the end repair process by the addition of a single 'A' base and the ligation of Illumina sequencing adapters.
442 The ligation products were selected by agarose gel electrophoresis, amplified by PCR, and sequenced using Illumina
443 HiSeq 4000 by Annoroad Technology (Beijing, China).
444

445 **Identification of DEGs.** The RPKM (reads per kb per million reads) method was used to calculate and normalize the
446 abundances of genes[60]. DEGs across groups were identified by the edgeR package (http://www.r-project.org/). Genes
447 with a fold change ≥ 2 and a false discovery rate (FDR) < 0.05 in a comparison were regarded as significantly expressed.
448 DEGs were then subjected to enrichment analysis of KEGG pathways.
449
450 **Viral infection *in vitro***. EPC, FG, or ZFL cells were plated 24 h before infection. Cells were infected with GCRV (5 ×
451 10^4TCID$_{50}$ per ml) or TSVDV (crude virus extracts filtered by a 0.45 μm microporous membrane) for 1 h in medium without
452 FBS. After infection, cells were washed with PBS and then medium was added with FBS. The cells and cell-free
453 supernatants were harvested at the indicated times.
454
455 **Viral infection *in vivo***. For *in vivo* viral infection, the adult WT and *bmp8a*$^{-/-}$ zebrafish were infected via intraperitoneal
456 injection using 50 μL of SVCV (10^8TCID$_{50}$ per ml), GCRV (10^8TCID$_{50}$ per ml), or TSVDV (crude virus extracts filtered by a
457 0.45 μm microporous membrane) per fish. Total RNA was extracted and viral RNA expression in the liver, kidney, intestine,
458 and spleen were examined by qRT-PCR. For the survival experiments, zebrafish were monitored for survival after SVCV,
459 GCRV, or TSVDV infection.
460
461 **Crystal violet staining**. EPC or ZFL cells were transfected with bmp8a or empty vector plasmid. At 24 h post transfection,
462 cells were treated with GCRV (5 × 10^4TCID$_{50}$ per ml). At 72 h after virus challenge, cells were fixed with 4% formaldehyde
463 for 1 h and stained with 0.5% crystal violet for 2 h. After washing with tap water, visible plaques were photographed.
464
465 **Luciferase assays.** EPC cells were seeded in 24-well plates overnight and cotransfected with various plasmids using
466 FuGENE HD Transfection Reagent (Promega, #E2311) following the manufacturer's instruction. If necessary, the cells
467 were infected with GCRV (5 × 10^4TCID$_{50}$ per ml). At the indicated time points, luciferase activities were measured with the
468 Luc-Pair Duo-Luciferase Assay Kits 2.0 (iGene Biotechnology, #LF002). Data were normalized by calculating the ratio
469 between firefly luciferase activity and *Renilla* luciferase activity. The primers used for cloning the promoter are shown in
470 Supplemental Table 2.
471
472 **RNA interference.** Small interfering RNA (siRNA) of bmp8a and si-NC (negative control) were purchased from RiboBio.
473 The oligonucleotide sequences (siRNA) specific targeting *bmp8a* mRNA was as follows: 5´-GTTCTTCAGAGCTAGTCAA-
474 3´. Transfection was performed with Lipofectamine RNAiMAX (Invitrogen, #13778075) according to the manufacturer's
475 protocols. Total RNA was extracted for qRT-PCR analysis.

476 **Drug treatment and analysis.** SMAD1/5/8 inhibitor DMH1(Selleck, #S7146), smad2/3 inhibitor TP0427736 HCl (Selleck,
477 #S8700), p38 MAPK inhibitor SB203580 (Beyotime, #S1863), JNK inhibitor SP600125 (Beyotime, #S1876), and MEK1/2
478 inhibitor U0126 (Beyotime, #S1901) were dissolved in dimethyl ulfoxide (DMSO). ZFL or EPC cells were treated with each
479 inhibitor, which were diluted with culture medium at concentrations of 10 μM for 24 h. Total cellular RNA was extracted for
480 qRT-PCR analysis.
481
482 **RNA quantification.** Total RNA was isolated using the miRNeasy Mini Kit (QIAGEN, #217004) according to the
483 manufacturer's instructions. RNA treated with DNase and the cDNAs were synthesized with PrimeScript™ RT reagent Kit
484 with gDNA Eraser (TaKaRa, #RP047A). Samples without reverse transcriptase were also added as control. Gene
485 expression was determined by amplifying the cDNA with ChamQ SYBR Color qPCR Master Mix(Vazyme, #Q431-02) by
486 an ABI 7500 Fast Real-Time PCR System (Applied Biosystems). The expression of zebrafish *actb1* or EPC *actin* was
487 used as an internal control. The $2^{-\Delta\Delta Ct}$ method was used to calculate relative expression changes. All qRT-PCR
488 experiments were performed in triplicate and repeated three times. Primers used are listed in Supplementary Table 1.
489
490 **Preparation of recombinant protein.** The recombinant protein of rStat1a or rStat1b was expressed and purified as
491 previous description[61]. Briefly, the recombinant plasmid (pET-28a-stat1a or pET-28a-stat1b) was transformed into *Trans*B
492 (DE3) chemically competent cell. The positive transformants were incubated in liquid LB medium containing 50 μg/mL
493 kanamycin at 37 °C by shaking at 160 rpm. When the cells grow to OD600 = 0.5, isopropyl β-D-thiogalactoside (IPTG)
494 was added to a final concentration of 1 mM, and incubated at 19 °C with shaking at 120 rpm for 14 h. After incubation, the
495 cells were harvested by centrifugation, re-suspended in PBS, and broken by ultrasound. The supernatant was centrifuged
496 at 12,000 g for 20 min, and the protein was purified by Ni-NTA Sepharose column. The concentration of purified protein
497 was determined by BCA (bicinchonininc acid) method. The purified recombinant proteins were stored at -80 °C for
498 subsequent experiment.
499
500 **Electrophoretic mobility shift assay.** Electrophoretic mobility shift assay (EMSA) was performed according to the
501 instruction of Chemiluminescent EMSA Kit (Beyotime, #GS009). Oligonucleotides (Supplementary Table 1) were
502 synthesized and biotinylated by Sangon Biotech Company as required and the complementary oligonucleotides were
503 annealed to form the double DNA probe. The recombinant protein was pre-incubated in EMSA/Gel-Shift binding buffer
504 with poly (dI-dC) at 25 °C for 25 min in the presence or absence of Non-Biotin probe (0.5 μM). Then, all samples were
505 mixed with biotinylated probes (0.5 μM) and incubated at 25°C for 30 min. The binding reaction without recombinant
506 protein was set as the negative control. For supershift analysis, anti-His tag antibody was incubated with the reaction

507 mixture for another 30 min after the labeled probe was added. After separation in a native 6% polyacrylamide gel, the free
508 probes and DNA-protein compound were transferred to a Hybond-N^+ nylon membrane, followed by crosslinking under UV
509 light. After immersion in the blocking buffer, membranes were incubated with streptavidin conjugated HRP for 20 min with
510 shaking and then washed three times with washing buffer. Membranes were exposed briefly in Western Lightning-ECL
511 and then exposure to Automatic X-ray Film Processor (Smpicgg).
512
513 **Immunoblot analysis and co-immunoprecipitation.** For Immunoblot analysis, cells were lysed in NP-40 buffer (150
514 mM NaCl, 0.5% EDTA, 50 mM Tris, 1% NP40, proteinase inhibitors, and protein phosphatase inhibitors) for 30 min on ice.
515 For co-immunoprecipitation (co-IP), whole-cell extracts were collected 48 h after transfection and lysed in NP-40 buffer on
516 ice for 30 min. After centrifugation for 15 min at 12,000 × g, 4 °C, supernatants were collected and incubated with Protein
517 A/G PLUS-Agarose (Santa Cruz, #sc-2003) coupled to specific antibodies for overnight with rotation at 4°C. Beads were
518 washed 3 × times with NP-40 buffer. Bound proteins were eluted by boiling 7min with 2 x SDS sample buffer. For
519 immunoblot analysis, immunoprecipitates or whole-cell lysates were separated by 12.5% SDS–PAGE gels, electro-
520 transferred to PVDF membranes and blocked for 4 h with 5% no-fat milk solution, followed by blotting with the appropriate
521 antibodies and detection by enhanced chemiluminiscence (ECL). Antibodies from Cell Signaling Technology: TBK1
522 (1:1000, #3504T), p-TBK1(Ser172) (1:1000, #5483T). Antibodies from Bioss: IRF3 (1:1000, #bs-2993R), p-IRF3 (Ser386)
523 (1:1000, #bsm-52170R), p38MAPK (1:1000, #bs-0637R), p-p38MAPK (Thr180 + Tyr182) (1:1000, #bs-2210R), Actin
524 (1:2000, #bs-0061R). Antibodies from Beyotime: HA tag (1:1000, #AH158) and Flag tag (1:1000, #AF519). Antibodies
525 from CWBIO: His tag (1:5000, #CW0285) and goat anti-rabbit IgG HRP secondary antibody (1:8000, #CW0103S).
526 Antibodies from Abcam: VeriBlot for IP Detection (1:5000, #ab131366).
527
528 **Statistical analysis and reproducibility.** Representative experiments have been repeated at least two to three times.
529 All statistical analysis was performed using Graphpad Prism 8.0.1. Data are presented as mean ± SEM. Statistical
530 significance was assessed using the unpaired, two-tailed Student's *t*-test. Survival analyses were performed using the
531 Kaplan-Meier method and assessed using the log-rank (Mantel-Cox) test. *$p < 0.05$, **$p < 0.01$, *** $p < 0.001$; ns, not
532 significant, $p > 0.05$.
533
534 **Data availability.** All data are available from the corresponding author upon reasonable request and that a Source Data
535 file is available for this article.
536

537 **References**

538 1. Thaiss, C. A., Levy, M., Itav, S. & Elinav, E. Integration of Innate Immune Signaling. *Trends Immunol*. **37**, 84-101
539 (2016).

540 2. Akira, S. & Hemmi, H. Recognition of pathogen-associated molecular patterns by TLR family. *Immunol*. *Lett*. **85**,
541 85-95 (2003).

542 3. Chen, S. N., Zou, P. F. & Nie, P. Retinoic acid-inducible gene I (RIG-I)-like receptors (RLRs) in fish: current
543 knowledge and future perspectives. *Immunology* **151**, 16-25 (2017).

544 4. Keating, S. E., Baran, M. & Bowie, A. G. Cytosolic DNA sensors regulating type I interferon induction. *Trends*
545 *Immunol*. **32**, 574-581 (2011).

546 5. Parvatiyar, K. et al. The helicase DDX41 recognizes the bacterial secondary messengers cyclic di-GMP and cyclic
547 di-AMP to activate a type I interferon immune response. *Nat*. *Immunol*. **13**, 1155-1161 (2012).

548 6. Zhou, P. et al. MLL5 suppresses antiviral innate immune response by facilitating STUB1-mediated RIG-I
549 degradation. *Nat*. *Commun*. **9**, 1243 (2018).

550 7. Honda, K. et al. IRF-7 is the master regulator of type-I interferon-dependent immune responses. *Nature* **434**, 772-
551 777 (2005).

552 8. Tamura, T., Yanai, H., Savitsky, D. & Taniguchi, T. The IRF family transcription factors in immunity and oncogenesis.
553 *Annu*. *Rev*. *Immunol*. **26**, 535-584 (2008).

554 9. Li, W., Hofer, M. J., Jung, S. R., Lim, S. L. & Campbell, I. L. IRF7-dependent type I interferon production induces
555 lethal immune-mediated disease in STAT1 knockout mice infected with lymphocytic choriomeningitis virus. *J*. *Virol*.
556 **88**, 7578-7588 (2014).

557 10. Schindler, C. & Plumlee, C. Inteferons pen the JAK-STAT pathway. *Semin*. *Cell Dev*. *Biol*. **19**, 311-318 (2008).

558 11. Decker, T., Kovarik, P. & Meinke, A. GAS elements: a few nucleotides with a major impact on cytokine-induced
559 gene expression. *J*. *Interferon Cytokine Res*. **17**, 121-134 (1997).

560 12. Fu, X. Y., Kessler, D. S., Veals, S. A., Levy, D. E. & Darnell, J. E. Jr. ISGF3, the transcriptional activator induced
561 by interferon alpha, consists of multiple interacting polypeptide chains. *Proc*. *Natl Acad*. *Sci*. *USA* **87**, 8555-8559
562 (1990).

563 13. Levy, D. E., Kessler, D. S., Pine, R. & Darnell, J. E. Jr. Cytoplasmic activation of ISGF3, the positive regulator of
564 interferon-alpha-stimulated transcription, reconstituted in vitro. *Genes Dev*. **3**, 1362-1371 (1989).

565 14. Levy, D. E., Kessler, D. S., Pine, R., Reich, N. & Darnell, J. E. Jr. Interferon-induced nuclear factors that bind a
566 shared promoter element correlate with positive and negative transcriptional control. *Genes Dev*. **2**, 383-393 (1988).

567 15. Ren, Y. et al. Deubiquitinase USP2a Sustains Interferons Antiviral Activity by Restricting Ubiquitination of Activated

568 STAT1 in the Nucleus. *PLoS Pathog*. **12**, e1005764 (2016).

569 16. Shuai, K., Schindler, C., Prezioso, V. R. & Darnell, J. E. Jr. Activation of transcription by IFN-gamma: tyrosine
570 phosphorylation of a 91-kD DNA binding protein. *Science* **258**, 1808-1812 (1992).

571 17. Bragdon, B., Moseychuk, O., Saldanha, S., King, D., Julian, J. & Nohe, A. Bone morphogenetic proteins: a critical
572 review. *Cell Signal* **23**, 609-620 (2011).

573 18. Crisan, M. et al. BMP signalling differentially regulates distinct haematopoietic stem cell types. *Nat*. *Commun*. **6**,
574 8040 (2015).

575 19. Wu, M., Chen, G. & Li, Y. P. TGF-beta and BMP signaling in osteoblast, skeletal development, and bone formation,
576 homeostasis and disease. *Bone Res*. **4**, 16009 (2016).

577 20. Xue, Y. et al. Organizer-derived Bmp2 is required for the formation of a correct Bmp activity gradient during
578 embryonic development. *Nat*. *Commun*. **5**, 3766 (2014).

579 21. Yu, Y., Mutlu, A. S., Liu, H. & Wang, M. C. High-throughput screens using photo-highlighting discover BMP signaling
580 in mitochondrial lipid oxidation. *Nat*. *Commun*. **8**, 865 (2017).

581 22. Huber, S. & Schramm, C. Role of activin A in the induction of Foxp3+ and Foxp3- CD4+ regulatory T cells. *Crit*.
582 *Rev*. *Immunol*. **31**, 53-60 (2011).

583 23. Martínez, V. G. et al. The canonical BMP signaling pathway is involved in human monocyte-derived dendritic cell
584 maturation. *Immunol*. *Cell Biol*. **89**, 610-618 (2011).

585 24. Martínez, V. G. et al. The BMP Pathway Participates in Human Naive CD4+ T Cell Activation and Homeostasis.
586 *PloS One* **10**, e0131453 (2015).

587 25. Phillips, D. J., de Kretser, D. M. & Hedger, M. P. Activin and related proteins in inflammation: not just interested
588 bystanders. *Cytokine Growth Factor Rev*. **20**, 153-164 (2009).

589 26. Seeger, P., Musso, T. & Sozzani, S. The TGF-β superfamily in dendritic cell biology. *Cytokine Growth Factor Rev*.
590 **26**, 647-657 (2015).

591 27. Takabayashi, H. et al. Anti-inflammatory activity of bone morphogenetic protein signaling pathways in stomachs of
592 mice. *Gastroenterology* **147**, 396-406 (2014).

593 28. Yasmin, N. et al. Identification of bone morphogenetic protein 7 (BMP7) as an instructive factor for human
594 epidermal Langerhans cell differentiation. *J*. *Exp*. *Med*. **210**, 2597-2610 (2013).

595 29. Sivertsen, E. A., Huse, K., Hystad, M. E., Kersten, C., Smeland, E. B. & Myklebust, J. H. Inhibitory effects and
596 target genes of bone morphogenetic protein 6 in Jurkat TAg cells. *Eur*. *J*. *Immunol*. **37**, 2937-2948 (2007).

597 30. Varas, A. et al. Interplay between BMP4 and IL-7 in human intrathymic precursor cells. *Cell cycle* **8**, 4119-4126
598 (2009).

599 31. Chen, W. & Ten Dijke, P. Immunoregulation by members of the TGFβ superfamily. *Nat*. *Rev*. *Immunol*. **16**, 723-740
600 (2016).
601 32. Zhao, G. Q., Deng, K., Labosky, P. A., Liaw, L. & Hogan, B. L. The gene encoding bone morphogenetic protein 8B
602 is required for the initiation and maintenance of spermatogenesis in the mouse. *Genes Dev*. **10**, 1657-1669 (1996).
603 33. Zhao, G. Q. & Hogan, B. L. Evidence that mouse Bmp8a (Op2) and Bmp8b are duplicated genes that play a role
604 in spermatogenesis and placental development. *Mech*. *Dev*. **57**, 159-168 (1996).
605 34. Walton, K. D. et al. Villification in the mouse: Bmp signals control intestinal villus patterning. *Development* **143**,
606 427-436 (2016).
607 35. Ying, Y., Qi, X. & Zhao, G. Q. Induction of primordial germ cells from murine epiblasts by synergistic action of BMP4
608 and BMP8B signaling pathways. *Proc*. *Natl Acad*. *Sci*. *USA* **98**, 7858-7862 (2001).
609 36. Zhong, S. j. et al. Spatial and temporal expression of *bmp8a* and its role in regulation of lipid metabolism in
610 zebrafish *Danio rerio*. *Gene Rep*. **10**, 33-41 (2018).
611 37. Robertsen, B. The interferon system of teleost fish. *Fish Shellfish Immunol*. **20**, 172-191 (2006).
612 38. Zhang, Y. B. et al. The innate immune response to grass carp hemorrhagic virus (GCHV) in cultured Carassius
613 auratus blastulae (CAB) cells. *Dev*. *Comp*. *Immunol*. **31**, 232-243 (2007).
614 39. Derynck, R., Akhurst, R. J. & Balmain, A. TGF-beta signaling in tumor suppression and cancer progression. *Nat*.
615 *Genet*. **29**, 117-129 (2001).
616 40. Drummond, A. E. TGFbeta signalling in the development of ovarian function. *Cell Tissue Res*. **322**, 107-115 (2005).
617 41. Oh, S. P., Yeo, C. Y., Lee, Y., Schrewe, H., Whitman, M. & Li, E. Activin type IIA and IIB receptors mediate Gdf11
618 signaling in axial vertebral patterning. *Genes Dev*. **16**, 2749-2754 (2002).
619 42. Shi, Y. et al. Exosomal Interferon-Induced Transmembrane Protein 2 Transmitted to Dendritic Cells Inhibits
620 Interferon Alpha Pathway Activation and Blocks Anti-Hepatitis B Virus Efficacy of Exogenous Interferon Alpha.
621 *Hepatology* **69**, 2396-2413 (2019).
622 43. Heldin, C. H., Miyazono, K. & ten Dijke, P. TGF-beta signalling from cell membrane to nucleus through SMAD
623 proteins. *Nature* **390**, 465-471 (1997).
624 44. Shi, Y. & Massagué, J. Mechanisms of TGF-beta signaling from cell membrane to the nucleus. *Cell* **113**, 685-700
625 (2003).
626 45. Worthington, J. J., Fenton, T. M., Czajkowska, B. I., Klementowicz, J. E. & Travis, M. A. Regulation of TGFβ in the
627 immune system: an emerging role for integrins and dendritic cells. *Immunobiology* **217**, 1259-1265 (2012).
628 46. Tu, E., Chia, P. Z. & Chen, W. TGFβ in T cell biology and tumor immunity: Angel or devil? *Cytokine Growth Factor*
629 *Rev*. **25**, 423-435 (2014).

630 47. Aleman-Muench, G. R. & Soldevila, G. When versatility matters: activins/inhibins as key regulators of immunity.
631 *Immunol. Cell Biol*. **90**, 137-148 (2012).
632 48. Bleul, C. C. & Boehm, T. BMP signaling is required for normal thymus development. *J. Immunol*. **175**, 5213-5221
633 (2005).
634 49. Gordon, J., Patel, S. R., Mishina, Y. & Manley, N. R. Evidence for an early role for BMP4 signaling in thymus and
635 parathyroid morphogenesis. *Dev. Biol*. **339**, 141-154 (2010).
636 50. Lee, M. K. et al. TGF-beta activates Erk MAP kinase signalling through direct phosphorylation of ShcA. *EMBO J*.
637 **26**, 3957-3967 (2007).
638 51. Itoh, S. et al. Trps1 plays a pivotal role downstream of Gdf5 signaling in promoting chondrogenesis and apoptosis
639 of ATDC5 cells. *Genes Cells* **13**, 355-363 (2008).
640 52. Wu, H., Zhang, Y., Lu, X., Xiao, J., Feng, P. & Feng, H. STAT1a and STAT1b of black carp play important roles in
641 the innate immune defense against GCRV. *Fish Shellfish Immunol*. **87**, 386-394 (2019).
642 53. Zou, J. & Secombes, C. J. Teleost fish interferons and their role in immunity. *Dev. Comp. Immunol*. **35**, 1376-1387
643 (2011).
644 54. Ruan, B. Y. et al. Two type II IFN members, IFN-γ and IFN-γ related (rel), regulate differentially IRF1 and IRF11 in
645 zebrafish. *Fish Shellfish Immunol*. **65**, 103-110 (2017).
646 55. Boehm, U., Klamp, T., Groot, M. & Howard, J. C. Cellular responses to interferon-gamma. *Annu. Rev. Immunol*.
647 **15**, 749-795 (1997).
648 56. Reed, L. J. & Muench, H. A Simple Method of Estimating Fifty Percent Endo-Points. *Am. J. Hyg*. **27**, 493-797
649 (1938).
650 57. Huang, P., Xiao, A., Tong, X., Zu, Y., Wang, Z. & Zhang, B. TALEN construction via "Unit Assembly" method and
651 targeted genome modifications in zebrafish. *Methods* **69**, 67-75 (2014).
652 58. Feng, H., Zhang, Y. B., Zhang, Q. M., Li, Z., Zhang, Q. Y. & Gui, J. F. Zebrafish IRF1 regulates IFN antiviral
653 response through binding to IFNϕ1 and IFNϕ3 promoters downstream of MyD88 signaling. *J. Immunol*. **194**, 1225-
654 1238 (2015).
655 59. Sun, F., Zhang, Y. B., Liu, T. K., Shi, J., Wang, B. & Gui, J. F. Fish MITA serves as a mediator for distinct fish IFN
656 gene activation dependent on IRF3 or IRF7. *J. Immunol*. **187**, 2531-2539 (2011).
657 60. Mortazavi, A., Williams, B. A., McCue, K., Schaeffer, L. & Wold, B. Mapping and quantifying mammalian
658 transcriptomes by RNA-Seq. *Nat. Methods* **5**, 621-628 (2008).
659 61. Sun, C., Hu, L., Liu, S., Gao, Z. & Zhang, S. Functional analysis of domain of unknown function (DUF) 1943,
660 DUF1944 and von Willebrand factor type D domain (VWD) in vitellogenin2 in zebrafish. *Dev. Comp. Immunol*. **41**,

469-476 (2013).

62. Qin, L., Wang. Y. G. & Zhang, Z. Multiple verrucous protrusions on skin in turbot Scophthalmus maximus. *J. Dalian Ocean Univ*. **23**, 479-483 (2008) (in Chinese with English abstract).

Author contributions

Z.L.and S.-C.Z. conceived and coordinated the project. Z.L., G.J., and S.Z. designed the experiments. S.Z., H.L. and Y.-S.W. performed experiments. H.-Y.L. and Y.W. contributed to establish the *bmp8a* knockout mutant lines (*bmp8a*$^{-/-}$) using TALENs technology. S.Z. performed the statistical analysis. Z.L., S.-C.Z. and S.Z. wrote the manuscript, with input from the other authors. All authors reviewed the manuscript and approved the final version.

Acknowledgements

This work was supported by the grants of National Natural Science Foundation of China (31572259) and National Key Research and Development Project of the Ministry of Science and Technology（2018YFD0900505）.

Conflict of Interest

The work is under a patent in China “A method to improve the antiviral immunity of fish (Application No. 201910454499.6)”.